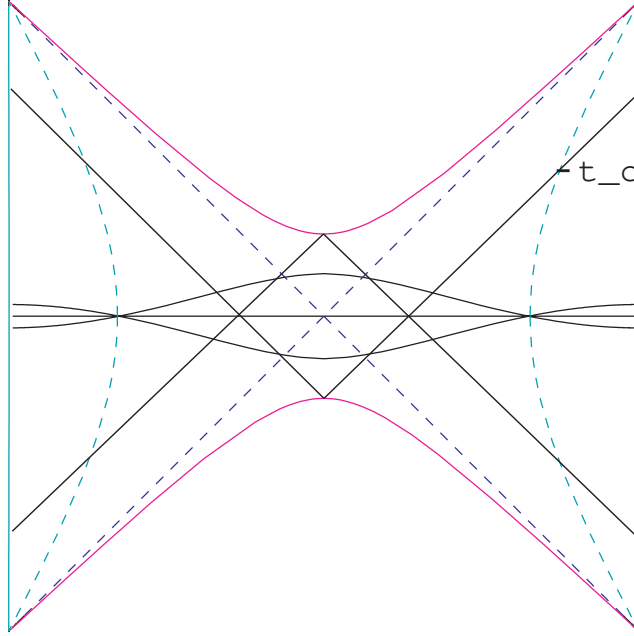


# D-Brane Instability as a Large N Phase Transition

Lukasz Fidkowski and Stephen Shenker

*Department of Physics, Stanford University, Stanford, CA, 94305, USA*

In AdS/CFT analyticity suggests that certain singular behaviors expected at large 't Hooft coupling should continue smoothly to weak 't Hooft coupling where the gauge theory is tractable. This may provide a window into stringy singularity resolution and is a promising technique for studying the signature of the black hole singularity discussed in hep-th/0306170. We comment briefly on its status. Our main goal, though, is to study a simple example of this technique. Gross and Ooguri (hep-th/9805129) have pointed out that the D-brane minimal surface spanning a pair of 't Hooft loops undergoes a phase transition as the distance between the loops is varied. We find the analog of this behavior in the weakly coupled Super Yang Mills theory by computing 't Hooft loop expectation values there.



**Fig. 1:** The Penrose diagram for the AdS-Schwarzschild black hole in  $d = 5$ . We have drawn the three geodesics connecting points with  $t = 0$  on the two asymptotic boundaries (at finite AdS cutoff), and the null  $t_c$  geodesic.

## 1. Introduction

In [1] we and our collaborators used the AdS/CFT correspondence to identify a subtle but distinct signature of the black hole singularity in a boundary thermal gauge theory correlator. This work built on earlier insights into studying physics behind the horizon using boundary correlators in AdS/CFT [2,3,4,5,6].<sup>1</sup> In [1] we studied boundary operators  $\mathcal{O}$  in D=4 SYM that create D3-branes in the  $\text{AdS}_5 \times S^5$  bulk wrapped on the  $S^5$  [8,9,10]. These behave like pointlike particles in the  $\text{AdS}_5$  space. The mass  $m$  of these particles is  $\sim N$  and so in the large  $N$  limit becomes infinite. In the bulk, correlators of these operators can be computed precisely in the supergravity limit by using the geodesic approximation,  $\langle \mathcal{O}(x)\mathcal{O}(y) \rangle \sim \exp(-m\mathcal{L})$  where  $\mathcal{L}$  is the proper length of the geodesic connecting  $x$  and  $y$ . In [1] we examined correlators of two such operators, one placed on each of the two disjoint boundaries of the eternal AdS-Schwarzschild black hole spacetime [4] (Fig.1). Even though these operators are spacelike separated their expectation value is bulk diffeomorphism invariant. This is different than the situation in asymptotically flat spaces where the only available diffeomorphism invariant quantities are S-matrix elements, which involve timelike or null separated sources. This subtlety of asymptotically AdS spaces opens up an important window. Geodesics between these points (Fig.1) pass behind the black hole horizon and so their behavior yields information about the geometry there.

<sup>1</sup> For subsequent work see [7].

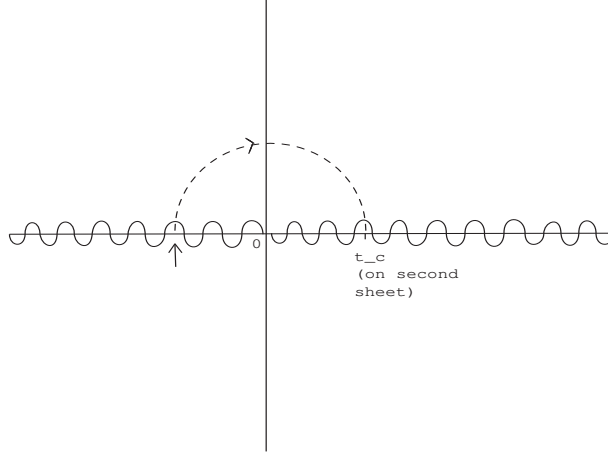


**Fig. 2:** The analytic structure of  $\mathcal{C}(t)$  in the complex  $t$  plane. The horizontal axis corresponds to Minkowski time, the vertical axis to Euclidean . There is a periodic identification  $t = t + i\beta$  in the  $t$  plane.  $t = i\frac{\beta}{2}$  corresponds to coincident points and the branch cut there (not shown) reflects the usual coincident points pole in  $\mathcal{C}(t)$ . Near 0,  $\mathcal{C}(t)$  has a  $t^{\frac{4}{3}}$  branch cut and the singularity corresponding to the null geodesic is at  $t_c$  on the second sheet. One gets to it by analytically continuing around the branch cut by 180 degrees, as indicated.

In fact it is possible to “move” an operator from one asymptotic boundary to another by analytically continuing in complexified boundary time  $t$ . All correlators are periodic with period  $i\beta$  where  $\beta$  is the inverse temperature of the black hole. Moving from one boundary to another involves shifting  $t \rightarrow -t + i\beta/2$ . So the correlator we are interested in can be represented as a thermal correlator  $C(t) = \langle \mathcal{O}(t)\mathcal{O}(-t + i\beta/2) \rangle$ . In fact, it will be more convenient to work with  $\mathcal{C}(t) = \log C(t)/m$ . The analytic structure of  $\mathcal{C}(t)$  determined in [1] is summarized in Fig.2. There is a cube root branch cut at  $t = 0$  that results from the coincidence of three geodesics linking the boundary points. Two of these geodesics “annihilate” and then become complex, much like roots of an analytic equation. On the second sheet, the correlator becomes dominated by a geodesic that at a certain  $t = t_c$  “bounces” off the black hole singularity when the geodesic is nearly null (Fig.1). The vanishing of its proper length means  $\mathcal{C}(t) \sim -2 \log(t - t_c)$ . This  $t_c$  singularity is a direct consequence of the diverging curvature at the black hole singularity and so provides a distinct signature of it in the boundary theory. The analysis described above is done in the supergravity limit,  $g_s, l_s \rightarrow 0$  or  $\lambda, N \rightarrow \infty$ , where  $l_s$  is the string length and  $\lambda$  is the ’t Hooft coupling.

The boundary gauge theory defined conventionally would actually yield results described by the first sheet in Fig.2. Here the bulk correlator is dominated for general  $t$  by complexified geodesics. But knowledge of these correlators on the first sheet is enough to

determine the behavior of  $\mathcal{C}(t)$  on the second sheet. A modest number of terms in a Taylor expansion of  $\mathcal{C}(t)$  allows one to determine  $t_c$  and the strength of the singularity there with high accuracy by standard extrapolation techniques. The singularity at  $t_c$  is a bit like a broad resonance and so its presence is reflected in a distinct but broad feature on the first sheet.<sup>2</sup>

In principle we could determine the effects of small but finite  $l_s$  ( $\alpha'$ ) on the black hole singularity by obtaining boundary gauge theory data at finite but large  $\lambda$  and extrapolating to the  $t_c$  singularity.<sup>3</sup> But we encounter the standard problem in employing dualities. The gauge theory at large  $\lambda$  is not effectively computable by gauge theory techniques.

But here we can take advantage of the severity of the problem we are studying. The black hole singularity is sufficiently mysterious that we would be happy to learn even something qualitative about its behavior. We expect the large  $N$  classical behavior of the gauge theory to be analytic in  $\lambda$  except at  $\lambda = \infty$ . The small  $\lambda$  expansion has a finite radius of convergence since there are only an exponential number of planar Feynman diagrams at each order. As  $\lambda \rightarrow \infty$  the tree level string dual has an asymptotic expansion in  $\alpha' \sim 1/\lambda^{1/2}$ . World sheet instantons produce effects of the form  $\exp(-1/\alpha') \sim \exp(-\lambda^{1/2})$  and we expect an essential singularity at  $\lambda = \infty$ . The analyticity tells us that if the  $t_c$  singularity persists to finite large  $\lambda$  (at  $g_s = 0$ ) then it must evolve analytically all the way to  $\lambda = 0$ . It can collide with other singularities and move off into the complex plane but it cannot just vanish. So the qualitative aspects of the singularity can be examined at small  $\lambda$ . Here weak coupling Feynman diagram techniques are effective. The presence of an essential singularity at  $\lambda = \infty$  allows the  $t_c$  singularity to vanish abruptly there, and be absent for all finite  $\lambda$ . This can be diagnosed at weak coupling.

This procedure of following large  $\lambda$  singularities to the small  $\lambda$  limit has been employed in the study of the Hawking-Page transition to the black hole [11,12]. In the gauge theory this is just a large  $N$  “deconfinement” transition. The Gregory-Laflamme transition has been described in a similar way [14,15].

The situation we are studying here is somewhat different because we are in the high temperature, “large black hole”,  $N^2$  entropy phase of the gauge theory for all  $\lambda$ . There

---

<sup>2</sup> This technique depends on the analyticity of various quantities. One might argue that we should just take the metric, computed outside the horizon, and analytically continue it to the singularity. This would be a reasonable thing to do except for the fact that in string theory the local metric is not meaningful. The virtue of the present approach is that we have located a signature of the black hole singularity in a system where all quantities are nonperturbatively well defined and analytic.

<sup>3</sup> Finite  $g_s$  is more subtle because the mass  $m \sim \lambda/g_s$  must be held larger than all other quantities. Certain quantities, like power series in  $g_s$ , leading nonperturbative effects, and certain scaling limits should be available, though [1].

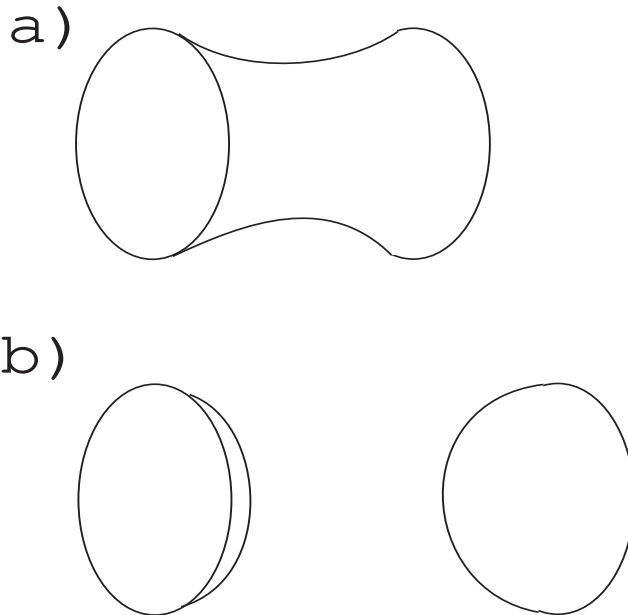


**Fig. 3:** (a) For  $s < s_0$ , the connected catenoid dominates. (b) For  $s > s_0$ , the disconnected disc solution dominates.

is no bulk phase transition. Instead we are looking at the dynamics of a single D-brane. This will involve  $N$  rather than  $N^2$  degrees of freedom.

The most straightforward singularity to study is not the  $t_c$  singularity but the branch cut at  $t = 0$  involving the coalescence of D-brane geodesics (Fig.1).

In this paper we study a “practice problem” where there is a coalescence of D-brane saddle points involving only  $N$  degrees of freedom and track it to small  $\lambda$ .

The problem we study was first described by Gross and Ooguri [16,17]. It involves the correlator of two ’t Hooft loops in the boundary gauge theory at zero temperature. In the bulk this correlator is determined by the world sheets of D-strings that end on the ’t Hooft loop. The tension of the D-string world sheet is  $l_s^2/g_s \sim N/\lambda^{1/2}$ . At infinite  $N$  the tension is infinite, independent of  $\lambda$ , so we can use saddle point techniques to pick out the dominant world sheet.<sup>4</sup> Consider circular loops of radius  $R$  oriented face to face with separation  $L$ . By conformal invariance things will depend only on the ratio  $s = L/R$ . For  $s \ll 1$  the dominant saddle is a catenoid connecting the loops. At  $s = s_0$  another saddle becomes dominant: two disconnected discs one terminating on each loop (see Fig.3). This “phase transition” is first order. The catenoid continues to exist for  $s > s_0$ , analogous to a metastable phase. Its properties can be studied by analytic continuation from the  $s < s_0$  regime. At  $s = s_1 > s_0$  the catenoid solution ceases to exist. Another catenoid, a local

---

<sup>4</sup> Gross and Ooguri also discuss the Wilson loop correlator. At any finite  $\lambda$  the fundamental string tension is finite so the transitions discussed below are smoothed out.

maximum of the action, coalesces with the stable catenoid and they both go off into the complex plane, analogous to a second order phase transition. The radius of curvature of these surfaces is of order  $L$  at the phase transitions, which can be taken much greater than the AdS radius which in turn is much greater than the string length at large  $\lambda$ . So we do not expect  $\alpha'$  effects to destabilize these transitions at large but finite  $\lambda$ . So we expect them to move analytically all the way to small  $\lambda$ .

Our main calculational goal in this paper is to study these phase transitions at weak gauge coupling. More precisely we will study the correlator of two 't Hooft loops at  $N = \infty$  and small  $\lambda$  where semiclassical techniques in the gauge theory are applicable. We find that at small  $\lambda$  the two phase transitions have merged into a second order transition occurring at a critical separation  $s_0(\lambda)$ . The small  $\lambda$  large  $N$  Feynman diagram analysis also suggests a connection between the second order transition and the strong coupling D-brane picture.

## 2. Construction of the 't Hooft Loop

Let us introduce some conventions. We will be working with the Euclidean  $\text{AdS}^5 \times S^5$  metric:

$$ds^2 = \frac{R^2}{Y^2} \left( \sum_{\mu=0}^3 dX^\mu dX^\mu + \sum_{i=1}^6 dY^i dY^i \right) \quad (2.1)$$

with the AdS radius  $R$  given by  $R^4 = \lambda \alpha'^2$  and  $Y^2 = \sum_{i=1}^6 Y_i^2$ . The dual gauge theory is  $\mathcal{N} = 4$  SYM, which in addition to the gauge fields has six scalars  $\Phi_i$ ,  $i = 1, \dots, 6$ , all in the adjoint. The bosonic part of the action is

$$S = \frac{1}{2g^2} \int d^4x \text{Tr} \left( \frac{1}{2} F_{\mu\nu} F^{\mu\nu} + \sum_{i=1}^6 (D_\mu \Phi_i)^2 + \sum_{1 \leq i < j \leq 6} [\Phi_i, \Phi_j]^2 \right) \quad (2.2)$$

The gauge theory supersymmetric Wilson loop operator

$$W(\mathcal{C}) = \text{Tr} \left[ P \exp \int_{\mathcal{C}} \left( i A_\mu \dot{x}^\mu + \theta^I \Phi^i \sqrt{\dot{x}^2} \right) d\tau \right] \quad (2.3)$$

can be evaluated in the bulk by integrating over fundamental string worldsheets attached to the the Wilson loop, weighted by  $\exp(-S)$  where  $S$  is the Polyakov action [18]. As discussed above, the tension of the fundamental string world sheet is finite for finite  $\lambda$  so all phase transitions are smeared out. For this reason we focus on 't Hooft loops, which are the electric-magnetic duals of Wilson loops and are evaluated in the bulk using D-string worldsheets, whose tension is proportional to  $N$ , and hence can be taken infinite independent of  $\lambda$ . We can write out the gauge theory operator corresponding to a 't Hooft

loop just by replacing the gauge field with its electric magnetic dual. To actually evaluate it (at small  $\lambda$ ) we follow the original construction.

The 't Hooft loop was originally defined [19] in an arbitrary Yang-Mills theory all of whose fields are invariant under the center  $Z_N$  of  $SU(N)$ . Before we discuss the loop, let's consider the simpler case of the 't Hooft vortex in  $2 + 1$  dimensional Yang Mills, also defined in [19]. The vortex can be thought of as a monopole in 3 dimensions. More precisely, we define the vortex operator  $\phi(x, t)$  in the Minkowski theory as an operator which acts on each field configuration by a multivalued gauge rotation whose holonomy around the point  $x$  is  $e^{\frac{2\pi i}{N}}$ , which is in the center  $Z_N$ . Then the computation of the correlator of these operators amounts to a path integral over field configurations with Dirac strings running between the vortex operators. For example, the two point function of  $\phi$  and  $\phi^*$  is given by

$$(\phi(0, t)\phi^*(0, 0)) = \frac{\int_C e^{-S}}{\int e^{-S}} \quad (2.4)$$

where the integral in the numerator is over all field configurations with a Dirac string running from one vortex to the other. The holonomy of the gauge field around the Dirac string is  $e^{\frac{2\pi i}{N}}$ . Thus in the saddle point approximation the logarithm of the two point function is the energy of two monopoles with opposite charges separated by a distance  $t$  in 3 dimensions.

The 't Hooft loop is the analog in  $3 + 1$  dimensions of the 't Hooft vortex, and the expectation value of a product of such loops is computed by doing a path integral over all field configurations with appropriate 2 dimensional Dirac sheets connecting the loops.

In order to evaluate the 't Hooft loop, we are instructed to do a path integral with certain boundary conditions at the Dirac worldsheet. Now, as 't Hooft [19] argues, the lowest action configurations will be ones in which the gauge field is that of a monopole whose world line is the loop and which lies in some  $U(1)$  that is conjugate in the  $SU(N)$  Lie algebra to the  $U(1)$  of the form  $\text{diag}(N - 1, -1, \dots, -1)$ . This is consistent with the holonomy condition. After we normalize and take the large  $N$  limit, these  $U(1)$ 's are basically all  $SU(N)$  conjugates of  $\text{diag}(1, 0, \dots, 0)$ . This set of matrices is just  $SU(N)/(U(1) \times SU(N - 1)) = CP^{N-1}$ . We denote this space  $M$ . It will be very useful to us in the rest of this paper. We note that we can parametrize it by matrices of the form  $\mathcal{M}_{ij} = (u_i u_j^*)$  where  $\sum u_i u_i^* = 1$ . The choice of  $u_i$  is unique except for an overall phase, and the parametrization in fact defines an  $S^1$  fibration  $S^{2N-1} \rightarrow CP^{N-1}$ . Also note that while  $M$  captures all of the possible boundary conditions for the 't Hooft loop, its adjoint has boundary conditions which can lie in any  $U(1)$  conjugate to  $\text{diag}(-1, 0, \dots, 0)$ . These boundary conditions are entirely disjoint from the original  $M$ , i.e. the set of  $SU(N)$  conjugates of  $\text{diag}(1, 0, \dots, 0)$  and  $\text{diag}(-1, 0, \dots, 0)$  comprise two disjoint copies of  $M$ . We refer to the adjoint boundary conditions as having negative gauge charge.

The loop also sources a scalar field, which one might think can be in any  $U(1)$ . However, if the state is not BPS then even though it has the same tree level energy as a BPS state, it gets infinite radiative corrections as the cutoff (i.e. the "thickness" of the monopole) is taken to zero. Thus we only need to consider BPS states. Setting the variation of the gaugino to zero, we have that the condition for unbroken supersymmetry is  $\Gamma^{\mu\nu}F_{\mu\nu}\epsilon = 0$ , where  $\epsilon$  is a Dirac spinor. The classical solutions for a straight line are ([20])

$$F_{\hat{\theta}\hat{\phi}} = X^9 = \frac{\pi N}{r} \quad (2.5)$$

$$F_{\hat{\theta}\hat{\phi}} = -X^9 = \frac{\pi N}{r} \quad (2.6)$$

The BPS conditions reduce to

$$(\Gamma^{\hat{\theta}\hat{\phi}} + \Gamma^{r9})\epsilon = 0 \quad (2.7)$$

$$(\Gamma^{\hat{\theta}\hat{\phi}} - \Gamma^{r9})\epsilon = 0 \quad (2.8)$$

and are satisfied by half of the spinors  $\epsilon$  as one can easily check. We see in particular that the gauge field and scalar will always be in the same  $U(1)$ .

We would like to have some information about the solution for a circular 't Hooft loop. One could make general arguments to obtain this information, but we will just do an explicit conformal transformation to make the straight line into a circle of radius  $R$  that sits centered at the origin of the  $(x, t)$  plane. One finds that the necessary transformation is

$$(t, x, y, z) \rightarrow \frac{2R^2}{u^2 + R^2 + 2xR} \left( t, \frac{u^2 - R^2}{2R}, y, z \right) \quad (2.9)$$

where  $u^2 = t^2 + x^2 + y^2 + z^2$ . The  $U(1)$  solution for the straight line up to sign and numerical factors is  $F_{ij} = (x_i^2)^{-\frac{3}{2}} \epsilon_{ijk} x_k dx_i dx_j$  and  $X_9 = (x_i^2)^{-\frac{1}{2}}$ , where we have introduced the spatial indices  $i, j, k = 1, 2, 3$ . The image of this solution under the conformal transform is

$$F = \frac{4R^2}{(t^2 + x^2 + y^2 + z^2 + R^2)^3} \times \omega \quad (2.10)$$

$$\omega = (2xz)dx \wedge dy + (-t^2 - x^2 + y^2 + z^2 + R^2)dy \wedge dz + (2xy)dz \wedge dx + (2zt)dy \wedge dt - (2yt)dz \wedge dt \quad (2.11)$$

$$X^9 = \frac{2R}{t^2 + x^2 + y^2 + z^2 + R^2} \quad (2.12)$$

Notice that the field strength decreases as the fourth power of the distance, and the scalar as the square of the distance.



### 3. Two 't Hooft Loops

Now that we have these preliminaries out of the way, we can look at the correlator  $H(s) = -\frac{1}{N} \log(T_1 T_2^*)$  at small  $\lambda$ , where  $s = L/R$  as defined above. For concreteness we will work in a fixed gauge, e.g.,  $\partial^\mu A_\mu = 0$ .

As discussed above, we have a certain classical configuration corresponding to  $T_1$ ; the one corresponding to the adjoint  $T_2^*$  has negative gauge charge. It also has the same scalar charge. We will make the ansatz that the lowest action configuration for two loops has their boundary conditions in the same  $U(1)$  and is the sum of the individual loop solutions ([19]). Note that it is not strange that the two scalar charges should be the same, since like scalar charges attract.

The configurations that contribute to the path integral have boundary conditions at each loop, so we can divide the configurations up into sectors parametrized by  $M \times M$ , where we think of the two  $M$ 's as parametrizing the boundary conditions at the two loops. This way of parametrizing configurations is not canonical, since it makes use of the fact that we are working in a particular gauge, but will nevertheless be useful. For each point in  $M \times M$ , i.e. each choice of boundary conditions, there is a lowest action field configuration with those boundary conditions. When the boundary conditions are the same, the minimal configuration is just the sum of the individual 't Hooft loop solutions, as described above. When they are orthogonal, i.e. if  $\text{Tr}(AB) = 0$  for  $(A, B)$  in  $M \times M$ , the sum of the individual one 't Hooft loop solutions in those  $U(1)$ 's gives a minimum for the action. Note that in this case the action is independent of the separation between the loops. We will refer to the preceding two possibilities as "same  $U(1)$ 's" and "orthogonal  $U(1)$ 's" respectively.

We want to define a parameter which measures the relative orientation of the two  $U(1)$ 's.  $y = \text{Tr}(AB)$  for  $(A, B)$  in  $M \times M$  would seem to be a natural choice. Letting  $B = \text{diag}(1, 0, \dots, 0)$  for simplicity we get  $y = u_1 u_1^*$  in terms of the previously defined parametrization of  $CP^{N-1}$ . Thus  $y$  ranges from 1 to 0, with  $y = 1$  for same  $U(1)$ 's and  $y = 0$  for orthogonal  $U(1)$ 's; in particular, note that  $y$  is always positive. However,  $y$  is not a good coordinate on  $M \times M$  near orthogonal  $U(1)$ 's because it is easy to see that for any smooth path on  $M$  parametrized by some coordinate  $\tau$  and starting at a  $U(1)$  orthogonal to  $\text{diag}(1, 0, \dots, 0)$ , we have  $y(\tau)$  going like at least  $\tau^2$  for small  $\tau$ . In other words, the appropriate coordinate near orthogonal  $U(1)$ 's is in a sense the square root of  $y$ , so we define  $u = y^{\frac{1}{2}}$ .

We now give an intuitive description of the weak coupling behavior of  $H(s)$ . For small  $s$  it is favorable for the loops to take advantage of the attractive magnetic interaction energy between them and orient their monopoles in the same  $U(1)$ . That is  $u \sim 1$ . But as  $s$  increases the interaction energy decreases and the loops start taking advantage of the very large number of near orthogonal  $U(1)$  directions. Entropy begins to dominate. Because

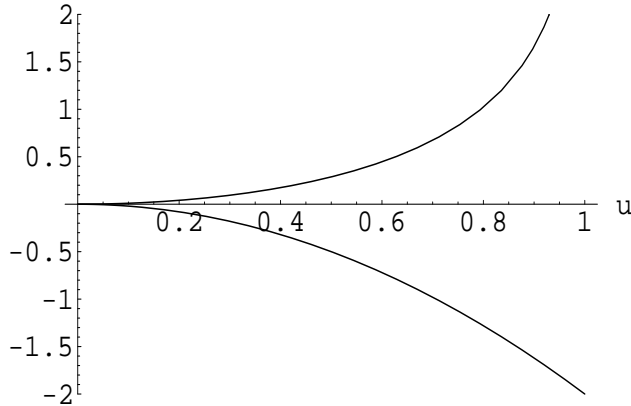


**Fig. 4:** A graph of the energy  $\mathcal{E}$  (lower line) and minus the entropy  $-S$  (upper line) as a function of  $u$  on  $M$ . The energy is maximized at the point of largest entropy.

$N$  is infinite this transition is sharp. After the transition the two  $U(1)$ 's are basically uncorrelated and so we would expect that  $H(s)$  is independent of  $s$ . This is reminiscent of the strong coupling picture, where after the transition to the disconnected caps  $H(s)$  becomes independent of  $s$  as well. We will discuss this connection in more detail below.

We now make our intuition precise. We define an effective action functional on  $M \times M$  by integrating over all field configurations with specified boundary conditions:

$$\exp(-Nf_{AB}) = \int_{AB} \exp(-S) \quad (3.1)$$

Here  $\int_{AB}$  is the path integral over configurations with boundary conditions  $A$  and  $B$  at the first and second 't Hooft loop respectively. Since  $f_{AB}$  depends only on  $u$ , we will use the notation  $f(u)$ . The tree level contribution to  $f_{AB}$  (denoted  $\mathcal{E}$ ) is just the action of the classical field configuration with those boundary conditions. For the regime we are interested in, namely large separation  $s$  and small coupling  $\lambda = g^2 N$ , the important,  $s$  dependent part of the action comes from points that are much farther away than  $R$  from either loop, and there the spacetime derivative term in the field strength dominates the commutator and so the sum is approximately a solution of the equations of motion. Its action is just proportional to  $u^2 = \text{Tr}AB$ . Higher order terms in  $u$  will come from corrections to the approximation we use and radiative corrections, suppressed by the coupling or the inverse separation. One can get the dependance on  $s$  using the  $r^{-2}$  fall off of the scalar at large distances, and obtain

$$\mathcal{E} = -\frac{N}{\lambda} c u^2 s^{-2} \quad (3.2)$$

where  $c$  is a numerical constant of order one.

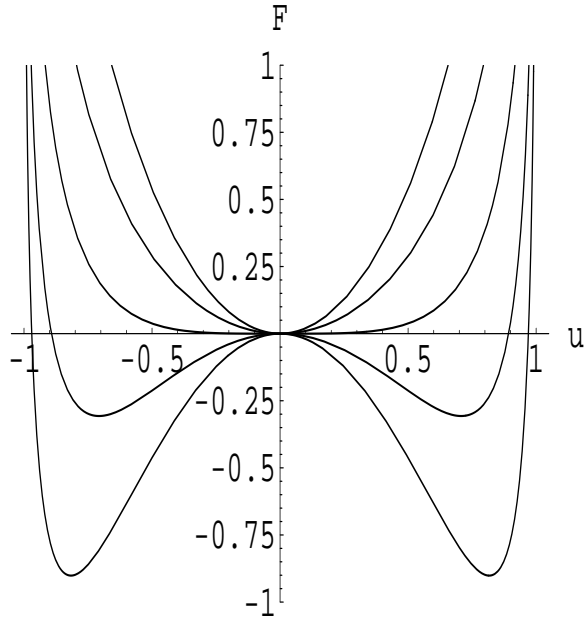


**Fig. 5:** A graph of the free energy  $f(u)$  for several values of the separation  $s$ . Note that for large  $s$  the value of  $u$  that minimizes  $F$  is 0. We have doubled the domain of  $u$  for clarity. The graph reflects the true nature of the transition near orthogonal  $U(1)$ 's on  $M \times M$ .

In addition to the tree level contribution, there are clearly many gauge field configurations with the same  $u$  so there is a large collective coordinate zero mode integral to do. (There are further nonzero mode radiative corrections but they are small at small  $\lambda$ . We discuss them later.) The integral over the zero modes (which can be associated with global gauge transformations) produces the entropy discussed above. The effective action functional with values of  $u$  between  $u$  and  $u + du$  gets weighted by an extra factor of  $\exp(\mathcal{S}(u))du$ , equal to the volume of  $M \times M$  between  $u$  and  $u + du$ . Here the volume is defined with respect to the unique metric on  $M \times M$  that is of product form and invariant under the  $SU(N)$  symmetry. In the large  $N$  limit

$$\mathcal{S}(u) = \frac{1}{2}N \log(1 - u^2). \quad (3.3)$$

This is just the entropy discussed above. The effective action at weak coupling (up to radiative corrections) is then just

$$Nf(u) = \mathcal{E} - \mathcal{S} = N\left(-\frac{1}{\lambda}cu^2s^{-2} - \frac{1}{2}\log(1 - u^2)\right) \quad (3.4)$$

The value of  $u$  that minimizes (3.4) is favored. At large  $N$  there are no fluctuations around this minimum.

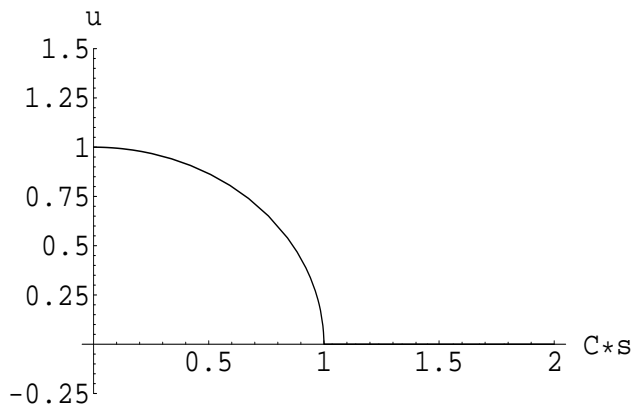


**Fig. 6:** A graph of the value of  $u$  that minimizes the free energy  $F$ , as a function of the separation  $s$ .

In Fig.5 we show how the profile of  $f$  changes as we vary  $s$  and in Fig.6 the resulting profile of the minimum  $u$ . We see that this is a standard second order phase transition with the coefficient of a quadratic minimum vanishing at some  $s = s_0(\lambda)$ . When  $s$  is near  $s_0(\lambda)$

$$f(u) = a_1(s - s_0(\lambda))u^2 + a_2u^4 + \dots \quad (3.5)$$

and because the expansion of  $-\log(1 - u^2)$  contains all *positive* order 1 coefficients, all the  $a_i$  are positive. Note that radiative corrections will have small coefficients (suppressed by  $\lambda$  and/or powers of the inverse separation) and so cannot change the nature of the transition. Thus indeed the transition is second order (i.e. the  $u$  that minimizes  $f(u)$  is a continuous function of  $s$ ). It follows that  $H(s)$  (the log of the 't Hooft loop correlator) goes like  $(s - s_0(\lambda))^2$  for  $s < s_0(\lambda)$  and is 0 for  $s > s_0(\lambda)$ . In fact,  $H(s)$  is *identically* 0, even including all radiative corrections. We explain this at the end of this section. To begin, we discuss general radiative corrections to (3.4).

First we argue qualitatively. The effective action expanded around a classical configuration like those discussed above will have the following schematic form

$$S_{eff} = N \int d^4x [A \text{Tr} F^2 + B \text{Tr} (DF)^2 + C \text{Tr} F^4 + \dots] \quad (3.6)$$

where  $F$  is the classical gauge field strength. We have omitted scalars for simplicity. The coefficient  $A$  vanishes because the beta function vanishes. The coefficients  $B$  and  $C$  are IR divergent. The natural IR cutoff is  $L$ , the separation between loops, so  $B \sim L^2$  and  $C \sim L^4$ .  $F$  goes like  $1/L^3$  so the second term is  $\sim 1/L^6$  and the third term is  $\sim 1/L^8$ . Both of these terms (and all others) are small compared to the leading classical term  $\sim \frac{1}{\lambda L^6}$ .

We will now give an argument that the coefficients in front of all terms in the effective action are finite to one loop. We find the fluctuation determinant using the background

field method, expanding about one of the classical solutions with some boundary conditions  $A, B$  at the two loops. The idea is to write the log of the determinant as in (3.6) and find the coefficients in front of all the terms using the standard 1PI Feynman diagram expansion. In fact we have separate determinants for the gauge field, scalar, and fermions. However, we can manipulate them to all look like determinants associated to Laplacians in some background (for the fermions we have to look at the square of the determinant), so that the final prescription becomes to sum over one loop diagrams with scalar propagators in the loop and background field insertions along it. Each momentum injected in an insertion is weighted by a factor equal to the fourier transform of the background field at that momentum, so that for each diagram we have to integrate over the loop momentum and over the external momenta. Let us consider a diagram with  $n$  insertions; it will be convenient to parametrize the momentum integrals by  $p_i, i = 1, \dots, n$ , where  $p_i$  is the momentum in the propagator between insertion  $i$  and  $i + 1$ . The diagram is then

$$\int \left( \prod_i d^4 p_i \right) \left( \prod_i \frac{1}{p_i^2} \right) \left( \prod_i B_i(p_i - p_{i+1}) \right) \quad (3.7)$$

where  $B$  is the fourier transform of one of the background fields. Let us look at potential IR divergences first. For small  $p$  we find, using the explicit one t' Hooft loop solution above, that  $B(p)$  goes like  $1/p^2$  for the scalar and like  $\log(p)$  for the gauge field strength. Only diagrams with all scalar insertions (and no scalar derivatives) could conceivably have an IR divergence and by general arguments these would not contribute to the  $s$ -dependent part of the effective action. In this particular theory we also know these vanish because of the existence of flat directions. The other diagrams are superficially IR convergent and in fact one can argue that they indeed are IR convergent. In the UV  $B(p)$  goes like  $1/p^2$  for both the gauge and scalar fields so the diagram is logarithmically UV divergent. However, because the two 't Hooft loop state is BPS on scales smaller than  $L$  this logarithmic divergence is cancelled and the diagram is superficially UV finite; again, one can argue that it actually is UV finite. We should note that potential  $UV$  divergences can come from integrations over the external momenta in addition to coming from the loop integral, and all diagrams have to be checked. Indeed, even the tree diagram corresponding to the classical action is UV divergent, reflecting the fact that the classical action of our configuration is infinite. The usual loop UV divergence, occuring in diagrams corresponding to  $F^2$  and  $(\partial X)^2$ , however, is cancelled just because of supersymmetry and does not rely on the BPS nature of the state.

When  $u = 0$  becomes the minimum, there is even more we can say - the radiative corrections, to all orders in perturbation theory, are zero in the large  $N$  limit. In other words, there are no planar diagrams in the expansion of the effective action about the orthogonal  $U(1)$ 's configuration. We argue as follows: take any 1PI loop diagram in

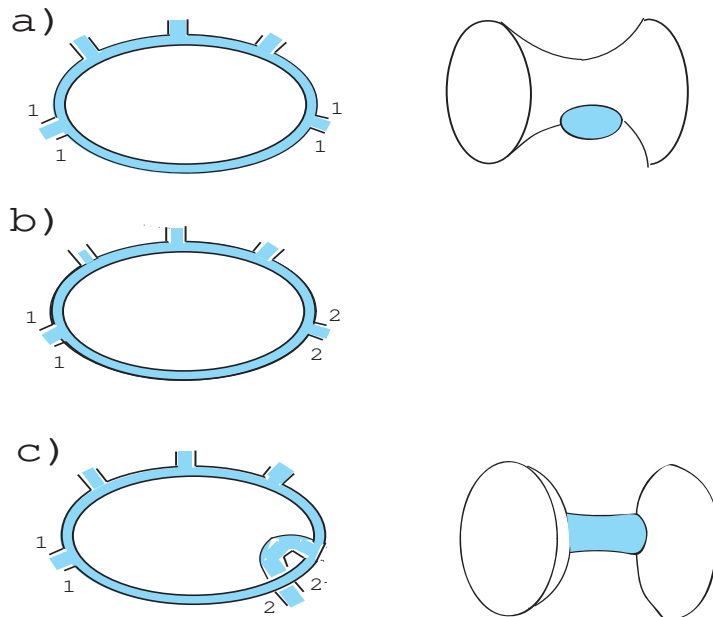


**Fig. 7:** (a) When the boundary conditions are not orthogonal, we can have type I and type II insertions from the same  $U(1)$  (among other possibilities). The resulting (leading in  $1/N$ ) radiative corrections correspond to disk worldsheets capping the connected  $U(1)$ 's configuration. (b) With orthogonal boundary conditions it is impossible to have radiative corrections that correspond to a worldsheet with disk topology. (c) Instead, the radiative corrections are down by a factor of  $N$  and correspond to worldsheets with cylindrical or higher genus topology connecting the two D-branes. There can be no disk worldsheets connecting two disconnected D-branes.

the expansion of the effective action around the classical orthogonal  $U(1)$ 's configuration and write it in fatgraph notation (see Fig.7). Because the background is the sum of two contributions coming from the two 't Hooft loops, we can separate the external insertions into two types, I and II, depending on which 't Hooft loop they came from. We can assume that the first  $U(1)$  is  $\text{diag}(1, 0, \dots, 0)$  and the second is  $\text{diag}(0, 1, \dots, 0)$ , so that the insertions in fatgraph notation will be  $(1, 1)$  and  $(2, 2)$ . The key point now is that any graph that has both type I and type II insertions cannot possibly be planar - if we interpret the graphs as worldsheets then type I and type II insertions cannot be put on the same boundary (because there would have to be some propagator that connects a type I and type II insertion, which is impossible, see Fig.7(b)). Note that this is true only for  $s > s_0(\lambda)$ ; for smaller  $s$  we do not have orthogonal  $U(1)$ 's and so it is possible to attach type I and type II insertions on the same boundary. This is suggestive because in the strong coupling picture the corrections to the 't Hooft loop correlator are given by F-string worldsheets ending on the D-brane; after the first order transition these worldsheets (at leading order in  $N$ ) turn

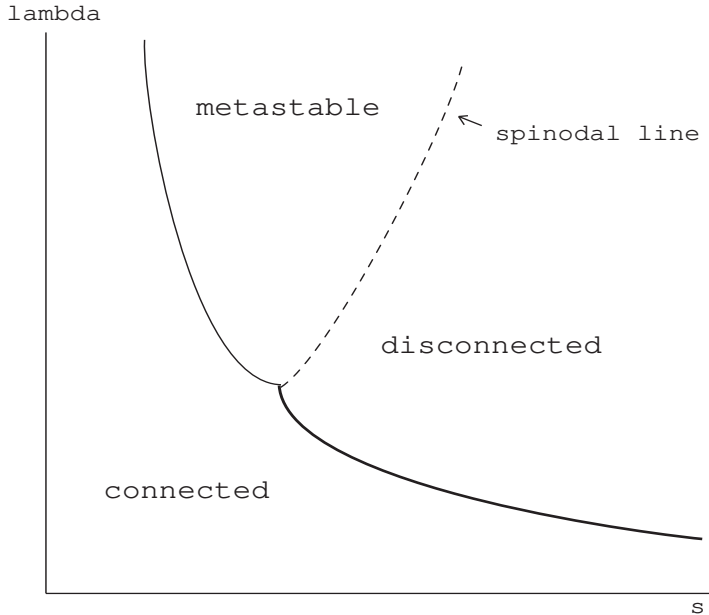


**Fig. 8:** Conjectured phase diagram in the  $s - \lambda$  plane. The light solid line is the line of first order transitions. The dotted line is the line of second order transitions in the metastable regime, the “spinodal line”. The heavy solid line is the line of second order transitions in the stable regime emerging from the tricritical point.

from disks to cylinders connecting the two D-string worldsheets (see Fig.7(c)). Thus we see that  $H(s)$  is constant, to all orders in  $\lambda$ , for  $s > s_0(\lambda)$ . Another way to see this is to use the fact that the state with orthogonal  $U(1)$ 's (which are orthogonal only to leading order in  $N$ ) is BPS to leading order in  $N$  and hence receives no radiative corrections.

We note that we could have attempted to do our entire analysis with static temporal 't Hooft loops at finite temperature. Here we would be working with Euclidean  $R^3 \times S^1$ ; [16] have shown that there exists strong coupling first and second order transitions in this case also. The computational advantages of working with this slightly simpler, static setup are offset by the fact that the gauge theory on  $R^3 \times S^1$  has bad infrared divergences. These occur at scales much longer than those relevant for our problem, so presumably our analysis would go through in some form.

#### 4. Discussion

We have found that the singular behavior of  $H(s)$  (the log of the 't Hooft loop correlator) retains some information about the phase transitions at strong coupling. The second order transition persists but the first order transition is absent. Assuming a low order polynomial approximation for  $f$  as in mean field theory we arrive at a natural conjecture

for the phase diagram in the  $(s, \lambda)$  plane (Fig.8). We conjecture that the first and second order transition lines at strong coupling merge at a tricritical point into a single line of second order transitions located at  $s_0(\lambda)$ . Here the loci of both first and order transitions vary analytically. In general this need not be the case because the location of a first order transition is determined by a *real* condition: that the real part of the effective actions of two saddle points agree.

As discussed in the Introduction an important application of these ideas is to the signature of the black hole singularity [1]. Here the branch cut at  $t = 0$  (Fig. 2) should continue to large finite  $\lambda$  as the scale of variation of the coalescing geodesics is AdS scale, much larger than string scale. So this singularity should move analytically all the way to small  $\lambda$ .

The operators that create wrapped D-branes are of the form  $\mathcal{O} = \det \phi^i$  where  $\phi^i$  is one of the SYM scalar fields [8,10]. The combinatorial formalism for evaluating correlators of  $\mathcal{O}$  in perturbation theory has been developed by Aharony, Antebi, Berkooz and Fishman [21]. In the simpler case where the gauge group is  $SO(2N)$  and the operator  $\mathcal{O} = \text{Pfaff} \phi^i$  their result is roughly the following (for large  $N$ ):

$$\begin{aligned} \langle \mathcal{O}\mathcal{O} \rangle &\sim \int \frac{d\beta}{\beta} e^{2Nf(\beta)} \\ f(\beta) &= \sum_{k \geq 1} \beta^k D_k - \frac{1}{2} \log \beta \end{aligned} \tag{4.1}$$

Here  $f(\beta)$  is a generating function and  $D_k$  denotes the sum over  $k$  particle irreducible diagrams. Parametrically  $D_k \sim \lambda^{k-1}$ . At large  $N$  (4.1) can be evaluated by finding saddle points of  $f(\beta)$ . Roughly speaking one balances the “entropy” of the many different ways one can break a diagram up into different subdiagrams against the “energy” of choosing the largest  $D_k$  values. In a thermal system in Minkowski time the  $D_k$  will oscillate and decay [22] allowing the possibility of multiple saddle points exchanging dominance. These are good candidates for the weak coupling image of the  $t = 0$  branch cut.

The dominant physics in such thermal correlators is efficiently summarized by a Boltzmann transport equation dominated by two body collisions occurring at a scattering rate  $\lambda^2 T$  where  $T$  is the temperature [22]. It is plausible that the effects of  $k$  body collisions described by  $D_k$  are suppressed relative to the two body collisions by a factor  $\lambda^{k-2}$ , uniformly in  $t$ . If this is the case then  $f(\beta)$  is convergent for all  $t$  and it is difficult to see an origin for the  $t_c$  singularity, where  $f$  should blow up. The  $D_k$  should each be finite at noncoincident points, disfavoring the  $\beta \sim 0$  singularity which dominates for coincident points. If these tentative observations are correct then the  $t_c$  singularity is not present at small  $\lambda$ . By analyticity this would mean that it has been smoothed out for all  $\lambda$  less than infinity. In other words, this signature of the black hole singularity would be resolved



purely by  $\alpha'$  effects, even at small  $\alpha'$ . This is surprising. We are continuing to investigate these issues.

## 5. Acknowledgements

We would like to thank Ofer Aharony, Matthew Kleban, Hong Liu, Xiao Liu, Juan Maldacena, Shiraz Minwalla, Hirosi Ooguri, Sergey Prokushkin, Soo-Jong Rey, Mohammed Sheikh-Jabbari, and Larry Yaffe for helpful discussions. This work was supported in part by NSF grant PHY-9870115 and the Stanford Institute for Theoretical Physics. The work of L. F. was supported in part by a National Science Foundation Graduate Research Fellowship.

## References

- [1] L. Fidkowski, V. Hubeny, M. Kleban and S. Shenker, “The black hole singularity in AdS/CFT,” *JHEP* **0402**, 014 (2004) [arXiv:hep-th/0306170].
- [2] V. Balasubramanian and S. F. Ross, “Holographic particle detection,” *Phys. Rev. D* **61**, 044007 (2000) [arXiv:hep-th/9906226].
- [3] J. Louko, D. Marolf and S. F. Ross, “On geodesic propagators and black hole holography,” *Phys. Rev. D* **62**, 044041 (2000) [arXiv:hep-th/0002111].
- [4] J. M. Maldacena, “Eternal black holes in Anti-de-Sitter,” arXiv:hep-th/0106112.
- [5] P. Kraus, H. Ooguri and S. Shenker, “Inside the horizon with AdS/CFT,” arXiv:hep-th/0212277.
- [6] T. S. Levi and S. F. Ross, “Holography beyond the horizon and cosmic censorship,” arXiv:hep-th/0304150.
- [7] V. Balasubramanian and T. S. Levi, “Beyond the veil: Inner horizon instability and holography,” arXiv:hep-th/0405048.
- [8] E. Witten, “Baryons and branes in anti de Sitter space,” *JHEP* **9807**, 006 (1998) [arXiv:hep-th/9805112].
- [9] J. McGreevy, L. Susskind and N. Toumbas, “Invasion of the giant gravitons from anti-de Sitter space,” *JHEP* **0006**, 008 (2000) [arXiv:hep-th/0003075].
- [10] V. Balasubramanian, M. Berkooz, A. Naqvi and M. J. Strassler, “Giant gravitons in conformal field theory,” *JHEP* **0204**, 034 (2002) [arXiv:hep-th/0107119].
- [11] E. Witten, “Anti-de Sitter space, thermal phase transition, and confinement in gauge theories,” *Adv. Theor. Math. Phys.* **2**, 505 (1998) [arXiv:hep-th/9803131].
- [12] B. Sundborg, “The Hagedorn transition, deconfinement and  $N = 4$  SYM theory,” *Nucl. Phys. B* **573**, 349 (2000) [arXiv:hep-th/9908001].
- [13] O. Aharony, J. Marsano, S. Minwalla, K. Papadodimas and M. Van Raamsdonk, “The Hagedorn / deconfinement phase transition in weakly coupled large  $N$  gauge theories,” arXiv:hep-th/0310285.
- [14] L. Susskind, “Matrix theory black holes and the Gross Witten transition,” arXiv:hep-th/9805115.
- [15] S. Minwalla, et al., to appear
- [16] D. J. Gross and H. Ooguri, “Aspects of large  $N$  gauge theory dynamics as seen by string theory,” *Phys. Rev. D* **58**, 106002 (1998) [arXiv:hep-th/9805129].
- [17] N. Drukker, D. J. Gross and H. Ooguri, “Wilson loops and minimal surfaces,” *Phys. Rev. D* **60**, 125006 (1999) [arXiv:hep-th/9904191].
- [18] O. Aharony, S. S. Gubser, J. M. Maldacena, H. Ooguri and Y. Oz, “Large  $N$  field theories, string theory and gravity,” *Phys. Rept.* **323**, 183 (2000) [arXiv:hep-th/9905111].
- [19] G. 't Hooft, “On The Phase Transition Towards Permanent Quark Confinement,” *Nucl. Phys. B* **138**, 1 (1978).

- [20] C. G. . Callan and J. M. Maldacena, “Brane dynamics from the Born-Infeld action,” Nucl. Phys. B **513**, 198 (1998) [arXiv:hep-th/9708147].
- [21] O. Aharony, Y. E. Antebi, M. Berkooz and R. Fishman, “‘Holey sheets’: Pfaffians and subdeterminants as D-brane operators in large N gauge theories,” JHEP **0212**, 069 (2002) [arXiv:hep-th/0211152].
- [22] See for example P. Arnold and L. G. Yaffe, “Effective theories for real-time correlations in hot plasmas,” Phys. Rev. D **57**, 1178 (1998) [arXiv:hep-ph/9709449].